ELSEVIER

S0032-3861(96)00366-7

Polymer Vol. 37 No. 22, pp. 5089–5097, 1996

0032-3861/96/$15.00 + 0.00

Temperature dependent elastic, piezoelectric and pyroelectric properties of β-poly(vinylidene fluoride) from molecular simulation

Jeffrey D. Carbeck and Gregory C. Rutledge*†
*Department of Materials Science and Engineering and *Department of Chemical Engineering, Massachussettes Institute of Technology, Cambridge, MA 02139, USA*
(Received 29 September 1995; revised 8 December 1995)

Detailed calculations of the elastic, piezoelectric and pyroelectric properties of the β phase of poly(vinylidene fluoride) are reported. The calculations are based on an empirical atomistic force field that uses the shell model of electronic polarization. Quasi-harmonic lattice dynamics is used to include the vibrational entropy in the calculation of the crystal free energy. The equilibrium crystal structure and polarization are determined as functions of temperature by minimization of the crystal free energy. The piezoelectric and pyroelectric responses are calculated by taking derivatives of the polarization with respect to strain and temperature, respectively. Changes in the unit cell volume dominate the piezoelectric and pyroelectric responses. Dipole oscillations make negligible contributions to the piezoelectric response. The primary pyroelectric response accounts for approximately 9% of the total pyroelectricity at 300 K. The temperature dependence of the piezoelectric stress coefficients is small. The temperature dependence of the piezoelectric strain coefficients is significant and correlates with the temperature dependence of the elastic compliance constants. Likewise, the temperature dependence of the pyroelectric response reflects that of the thermal expansion coefficients. Copyright © 1996 Elsevier Science Ltd.

(Keywords: poly(vinylidene fluoride); piezoelectricity; pyroelectricity; elasticity; simulation)

INTRODUCTION

Poly(vinylidene fluoride) in its β phase (β-PVDF) is a polar crystal[1]. Bulk, semi-crystalline films of β-PVDF are rendered polar through the process of poling in which the different crystalline regions are aligned along a common axis by the application of an electric field. Changes in the polarization with strain and temperature are described by the piezoelectric and pyroelectric coefficients, respectively[1]. The large piezoelectric and pyroelectric coefficients of β-PVDF films coupled with their mechanical properties have made these films a successful commercial material[2]. The piezoelectric and pyroelectric properties of semi-crystalline films of β-PVDF have been well characterized. However, the fundamental molecular mechanisms that give rise to these responses are still unclear[3,4]. This lack of resolution is due to the difficulty in directly probing the crystalline phase of semi-crystalline films—a frequently encountered problem in polymer physics. Molecular simulations can be useful for such problems as they can focus directly on the crystalline phase of the semi-crystalline film and provide details at the molecular level.

In polar crystals the piezoelectric response is a result of the coupling between the dielectric and the mechanical responses of the crystal. Likewise, the pyroelectric response includes a contribution from the coupling of the piezoelectric and thermal expansion coefficients[5]. A complete study needs to address the elastic responses, the thermal expansion and the polarization of the crystal in a consistent manner.

Previous attempts at calculating the piezoelectric and pyroelectric properties of β-PVDF fall into three general categories: (i) models based on simple continuum dielectric theory[6]; (ii) models based on the explicit lattice summations of idealized dipoles[7–11]; and (iii) models based on molecular simulations[12–14]. Models in categories (i) and (ii) require additional approximations of the crystal elastic properties and the thermal expansion coefficients whereas models in category (iii) can, in principle, be used to calculate these properties as well.

In a previous publication, referred to hereafter as Paper I, we presented a consistent model of the crystal polarization and local electric field in β-PVDF based on the minimum free energy crystal structure calculated using consistent quasi-harmonic lattice dynamics (CLD)[15]. In this paper, we extend this method to the determination of the piezoelectric and pyroelectric properties. This approach has several distinct advantages. First, the combination of an atomic-level description of the repeat unit electrostatics with the use of Ewald sums allows for a more thorough representation of the internal electric field effects in the crystal. Previous attempts at quantifying these effects were based on much

† To whom correspondence should be addressed

simpler representations of the repeat unit charge distribution, with the results being very sensitive to the details of the representation[7-11]. Second, this technique utilizes an empirical potential energy expression that includes the shell model of electronic polarization[14]. The use of this model allows for explicit inclusion of electronic polarization at the molecular level. Third, the inclusion of vibrational entropy in the crystal free energy expression allows for a direct determination of the crystal structure, polarization, dielectric constant, elastic stiffness and compliance constants, and thermal expansion coefficients as functions of temperature. All of these quantities play a part in the analysis of the piezoelectric and pyroelectric responses of β-PVDF. Finally, the normal-mode frequencies and eigenvectors give information about atomic motions in the crystal which can be utilized to include the effects of dipole oscillations in calculating the piezoelectric and pyroelectric properties of β-PVDF. The accuracy of this approach is limited by the parameterization of the empirical force field and the validity of the harmonic approximation.

THEORY

β-PVDF displays a non-zero polarization parallel to the b crystal axis; the components along a and c are zero due to the symmetry of the crystal. To maintain consistency with the literature on β-PVDF, we label c as the 1 axis, a as the 2 axis and b as the 3 axis, as shown in *Figure 1*. We report only the orthogonal tensile properties of the β-PVDF orthorhombic unit cell. In this work we use i and j to represent the principle indices in Voigt notation, and k and l to represent the principle Cartesian indices, x, y, z. The Einstein summation convention, which implies summation over repeated indices, is also utilized.

Model of crystal polarization

The polarization is defined as the dipole moment density of the crystal. In β-PVDF there are two identical chemical repeat units CH_2CF_2 per unit cell. Each repeat unit is aligned in the unit cell such that the repeat unit dipole is parallel to the 3 axis. Because of this arrangement, the polarization and repeat unit dipole can be represented as scalars and the polarization is written as

$$P_3 = \frac{2\mu}{V} \tag{1}$$

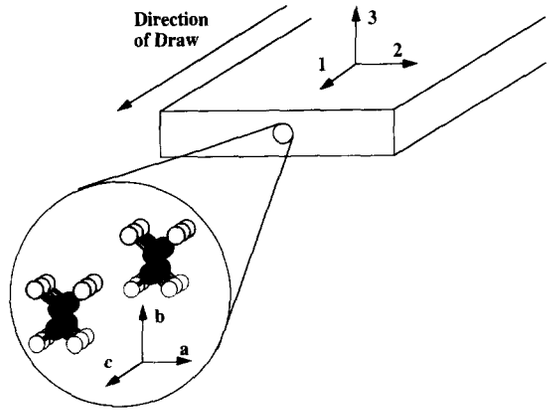

Figure 1 Relationship between film coordinates and unit cell coordinates in β-PVDF

where μ is the magnitude of the repeat unit dipole moment parallel to the 3 axis and V is the unit cell volume.

In Paper I we defined the total repeat unit dipole in the crystal as

$$\mu = \mu^{sc}\langle\cos\varphi\rangle + \Delta\mu \tag{2}$$

where μ^{sc} is the dipole of each repeat unit of the single chain in vacuum, $\Delta\mu$ is the change in repeat unit dipole in going from the single chain in vacuum to the packed crystal, and $\langle\cos\varphi\rangle$ is the attenuation of the repeat unit dipole due to thermal oscillations. $\Delta\mu$ is given by

$$\Delta\mu = \alpha E_{loc} \tag{3}$$

where α is the repeat unit polarizability along 3 and E_{loc} is the local electric field along 3, which arises—in the absence of an applied field—from the dipoles on the neighbouring chains in the crystal. (Contributions to the local electric field due to dipoles on the same chain are also present, but are not included in E_{loc}. These intramolecular contributions are already accounted for in μ^{sc}.) $\langle\cos\varphi\rangle$ is the ensemble averaged projection of the repeat unit dipole in the crystal along the 3 axis. In deriving equation (2) we made the approximation that only the single chain dipole is attenuated by thermal oscillations. The force field used in our calculations was based on the shell model which included both atomic and electronic polarization effects in determining μ^{sc}, $\Delta\mu$ and α. From equation (2) the crystal polarization parallel to the 3 axis is

$$P_3 = \frac{2}{V}(\mu^{sc}\langle\cos\varphi\rangle + \Delta\mu) \tag{4}$$

Elastic, piezoelectric and pyroelectric responses

In the case of polar crystals such as β-PVDF, the elastic and dielectric properties are coupled. If we take stress, σ_j, temperature, T, and applied electric field, E_k as the independent variables, then the dependent quantities are strain, ϵ_i, and polarization, P_k^σ,

$$\epsilon_i = S_{ij}\sigma_j + \alpha_i T + d_{ik}^c E_k \tag{5}$$

$$P_k^\sigma = d_{kj}\sigma_j + p_k^\sigma T + \chi_{kl}^\sigma E_l \tag{6}$$

where S_{ij} are the elastic compliance constants, α_i are the linear thermal expansion coefficients, d_{kj} and d_{ik}^c are the direct and converse piezoelectric strain coefficients, respectively, p_k are the pyroelectric coefficients, and χ_{kl} are the dielectric susceptibility constants. The superscript, σ, on P_k, p_k and χ_{kl} indicate that these quantities are defined for conditions of constant stress. If instead we take ϵ_j, T and E_k as the independent variables, then the dependent quantities are σ_i and P_k^ϵ

$$\sigma_i = C_{ij}\epsilon_j - f_i T + g_{ik}^c E_k \tag{7}$$

$$P_k^\epsilon = g_{kj}\epsilon_j + p_k^\epsilon T + \chi_{kl}^\epsilon E_l \tag{8}$$

where C_{ij} are the elastic stiffness constants, $-f_i$ are the thermal stress coefficients, and g_{kj} and g_{ik}^c are the direct and converse piezoelectric stress coefficients, respectively. The superscript, ϵ, on P_k, p_k and χ_{kl} indicate that these quantities are now defined for conditions of constant strain.

The coefficients appearing in equations (5)–(8) are

defined by the partial derivatives of the dependent variables with respect to the appropriate independent variables. In this way, from equation (5), the elastic compliance constants are defined as

$$S_{ij} \equiv \left(\frac{\partial \epsilon_i}{\partial \sigma_j}\right)_{T,E} \tag{9}$$

The linear and volume thermal expansion coefficients are defined as

$$\alpha_i \equiv \left(\frac{\partial \epsilon_i}{\partial T}\right)_{\sigma,E} = \frac{1}{a_i}\left(\frac{\partial a_i}{\partial T}\right)_{\sigma,E} \tag{10}$$

$$\alpha_V \equiv \frac{1}{V}\left(\frac{\partial V}{\partial T}\right)_{\sigma,E} \tag{11}$$

where a_i are the lattice parameters. For an orthorhombic unit cell, α_V is given as

$$\alpha_V = \alpha_1 + \alpha_2 + \alpha_3 \tag{12}$$

From equations (5) and (6), the converse and direct piezoelectric strain coefficients, d_{i3}^c and d_{3i}, are defined as

$$d_{i3}^c \equiv \left(\frac{\partial \epsilon_i}{\partial E_3}\right)_{T,\sigma} \tag{13}$$

$$d_{3i} \equiv \left(\frac{\partial P_3}{\partial \sigma_i}\right)_{T,E} \tag{14}$$

and from equations (7) and (8), the converse and direct piezoelectric stress coefficients, g_{i3}^c and g_{3i}, are defined as

$$g_{i3}^c \equiv \left(\frac{\partial \sigma_i}{\partial E_3}\right)_{T,\epsilon} \tag{15}$$

$$g_{3i} \equiv \left(\frac{\partial P_3}{\partial \epsilon_i}\right)_{T,E} \tag{16}$$

The direct piezoelectric strain and stress coefficients are related through the elastic compliance constants,

$$d_{ki} = S_{ij} g_{kj} \tag{17}$$

The pyroelectric coefficient at constant strain, p_3^ϵ, describes a change in polarization with temperature when the sample is effectively clamped. From equation (8), p_3^ϵ is defined as

$$p_3^\epsilon \equiv \left(\frac{\partial P_3}{\partial T}\right)_{\epsilon,E} \tag{18}$$

If the sample is instead allowed to change its shape and volume with changes in temperature, then the pyroelectric response is given by p_3^σ which from equation (6) is defined as

$$p_3^\sigma \equiv \left(\frac{\partial P_3}{\partial T}\right)_{\sigma,E} \tag{19}$$

p_3^σ can be written as a sum of p_3^ϵ and the product of the direct piezoelectric stress coefficient, g_{3i}, and the thermal strain given by the thermal expansion[5],

$$p_3^\sigma = p_3^\epsilon + g_{3i}\alpha_i \tag{20}$$

The total pyroelectric response at constant stress, p_3^σ, is the sum of the *primary* pyroelectric response, given by p_3^ϵ, and the *secondary* pyroelectric response, $g_{3i}\alpha_i$.

Because of the symmetry of the unit cell, only the polarization along the 3 axis is non-zero in β-PVDF. In this work, we do not consider any variations that break this symmetry; in evaluating the piezoelectric and pyroelectric responses we consider changes in polarization along the 3 axis only. Subscripts on partial derivatives are also omitted unless required for clarity. We obtain an expression for d_{3i} from our polarization model by evaluating equation (14) using equation (4)

$$d_{3i} = \frac{2\mu^{sc}}{V}\left(\frac{\partial\langle\cos\varphi\rangle}{\partial\sigma_i}\right) + \frac{2}{V}\left(\frac{\partial\Delta\mu}{\partial\sigma_i}\right) - P_3\sum_j S_{ij} \tag{21}$$

The g_{3i} are, likewise, obtained from our polarization model by evaluating equation (16) and equation (4)

$$g_{3i} = \frac{2\mu^{sc}}{V}\left(\frac{\partial\langle\cos\varphi\rangle}{\partial\epsilon_i}\right) + \frac{2}{V}\left(\frac{\partial\Delta\mu}{\partial\epsilon_i}\right) - P_3 \tag{22}$$

The pyroelectric coefficient at constant strain, p_3^ϵ given in equation (18), is expressed in the polarization model as

$$p_3^\epsilon = \frac{2\mu^{sc}}{V}\left(\frac{\partial\langle\cos\varphi\rangle}{\partial T}\right)_\epsilon \tag{23}$$

In the quasi-harmonic approximation, the term $(\partial\Delta\mu/\partial T)$ is zero at constant strain. From equation (20) the pyroelectric coefficient at constant stress, p_3^σ, is

$$p_3^\sigma = \frac{2\mu^{sc}}{V}\left(\frac{\partial\langle\cos\varphi\rangle}{\partial T}\right)_\epsilon + \alpha_i g_{3i} \tag{24}$$

COMPUTATIONS

In this work, the crystal polarization and its derivatives with temperature and strain are calculated using consistent quasi-harmonic lattice dynamics (CLD). This technique allows for the inclusion of the vibrational entropy in the calculation of the crystal free energy. CLD is based on a Taylor series expansion of the crystal potential energy given, in this work, by an empirical force field. In the harmonic approximation, the Taylor series is truncated after the second order term and the resulting differential equations have harmonic solutions. The dynamical equations can be transformed into normal-mode coordinates and the equations of motion then become those of a collection of non-interacting one-dimensional harmonic oscillators for which analytical expressions for both the classical and quantum mechanical partition functions are available. The Helmholtz vibrational free energy of the crystal, A_{vib}, is then calculated directly from the partition function. Quasi-harmonic lattice dynamics includes the anharmonicity due to changes in normal-mode frequency with lattice constants. The techniques of lattice dynamics are well developed and the reader is referred to several sources for further details[16,17]. A detailed explanation of CLD and its application to the calculation of the minimum free energy crystal structure and properties of poly(ethylene) has recently been published[18].

We use modified versions of the MSXX and MSXXS force fields developed by Karasawa and Goddard[14] (KG) which we denote MSXX* and MSXXS*. These force fields were used as reported, except for the fluorine van der Waals parameters. These were taken from crystalline F_2[19] and are given in *Table 1*, along with those originally reported by KG. The revised van der Waals parameters for fluorine were required to maintain

Table 1 Fluorine van der Waals parameters.

$$U_{vdW} = \frac{\epsilon_v}{\zeta - 6}[6\exp(\zeta(1-\rho)) - \zeta\rho^{-6}]; \rho = R/R_v$$

	R_v (Å)	ϵ_v (kcal mol^{-1})	ζ
This work	3.2000	0.0600	14
KG[a]	3.5380	0.0211	16

[a] Ref. 14

accurate estimations of the equilibrium lattice constants and vibrational stability in CLD. These modifications are described in further detail in Paper I. The MSXX* and MSXXS* force field differ in that the MSXXS* force field employs the shell model of electronic polarization while MSXX* employs the standard fixed partial atomic charge model. The Ewald summation method[20] is used to calculate the Coulombic and dispersion interactions with all sums carried out to an accuracy of 0.01 kcal mol^{-1}. Analytical second derivatives are used to determine the normal mode frequencies. The normal-mode frequencies are wave vector dependent and A_{vib} is obtained by integrating over the first Brillouin zone using Gauss–Legendre quadrature on a $4 \times 4 \times 4$ mesh. The total Gibbs free energy is then calculated from

$$G(T, \boldsymbol{\sigma}) = U(\mathbf{a}) + A_{vib}(T, \mathbf{a}) - V\sum_{i,j}\sigma_i\epsilon_j \qquad (25)$$

where $U(\mathbf{a})$ is the potential energy given by the force field for the set of lattice constants, **a**.

By minimizing $G(T, \boldsymbol{\sigma})$ with respect to the lattice constants, **a**, and positions of all atoms and shells within the unit cell, we determined the equilibrium free energy unit cell structure at each temperature (at zero applied stress). From this structure, the temperature dependent crystal polarization and repeat unit dipole were obtained directly. Values for $\langle\cos\varphi\rangle$ were obtained from the normal mode frequencies and eigenvectors of the B_2 rotational lattice mode at each temperature, as described in the Appendix. For the repeat unit dipole moment of the single chain in vacuum we used results from calculations of a single infinite chain with an axial repeat distance of 2.56 Å, reported in Paper I.

Thermal expansion coefficients were estimated from analytical derivatives of 4th-order polynomials fit to the lattice constants *versus* temperature between 0 and 400 K. Elastic constants and piezoelectric coefficients were determined from free energy minimizations at fixed strains of 0.25% about the equilibrium lattice constants at each temperature. We considered only tensile and compressive strains (i.e. $i, j = 1, 2, 3$) for a total of 24 additional free energy minimizations at each temperature. The elastic stiffness constants, C_{ij} $(i, j = 1, 2, 3)$ were then estimated numerically from the second derivatives of the crystal Helmholtz free energy, $A(T, \mathbf{a})$, with respect to strain. The elastic compliance constants, S_{ij} $(i, j = 1, 2, 3)$, were determined by inversion of the elastic stiffness tensor. For the orthorhombic lattice, **C** is block diagonal and it is not necessary to consider shear constants in order to obtain the desired values for S_{ij}. The direct piezoelectric stress coefficients, g_{3i} $(i = 1, 2, 3)$ as expressed in equation (22), were determined from the derivatives of $\Delta\mu$, which was estimated numerically, and of $\langle\cos\varphi\rangle$, which was calculated as described in the Appendix, each with respect to strain. From the piezoelectric stress coefficients and the elastic compliance constants, we determined the direct piezoelectric strain coefficients, d_{3i}, using equation (17). The constant strain pyroelectric coefficient, p_3^σ as expressed in equation (24), was calculated from the thermal expansion coefficients, piezoelectric stress coefficients and the derivative of $\langle\cos\varphi\rangle$—calculated as described in the Appendix—with respect to temperature.

RESULTS AND DISCUSSION

Thermal expansion and elasticity

The lattice constants and thermal expansion coefficients of β-PVDF are provided in *Table 2* as a function of temperature calculated using CLD and the MSXX* force field. The lattice constants are essentially unchanged with the use of the MSXXS* force field and are used as the equilibrium lattice constants throughout this work. α_2 and α_3 are positive and increase with temperature. α_1 is negative and an order of magnitude smaller than α_2 and α_3. Previous application of CLD to the calculation of the thermal expansion of poly(ethylene) gave results in very good agreement with experiment[18]. We are not aware of any experimental data for the thermal expansion of β-PVDF for comparison here. The negative axial thermal expansion, α_1, is similar to that observed in poly(ethylene) and arises in part from thermally induced compressive stresses along the chain axis, and Poisson coupling to the tensile thermal stresses lateral to the chain axis.

In *Table 2* we report the elastic stiffness constants calculated using the MSXX* force field and numerical derivatives of the crystal Helmholtz free energy,

$$C_{ij} = \frac{1}{V}\left(\frac{\partial^2 A}{\partial\epsilon_i\,\partial\epsilon_j}\right) = \frac{1}{V}\left(\frac{\partial^2 U}{\partial\epsilon_i\,\partial\epsilon_j}\right) + \frac{1}{V}\left(\frac{\partial^2 A_{vib}}{\partial\epsilon_i\,\partial\epsilon_j}\right) \qquad (26)$$

Similar results where obtained with the MSXXS* force field. In *Table 3* we indicate the potential energy, U, and vibrational free energy, A_{vib}, contributions to the elastic stiffness constants at 300 K according to equation (26). The elastic tensor demonstrates the characteristic anisotropy of extended chain polymer crystals, with the stiffness along the axial direction, 1, an order of magnitude larger than the values transverse to the chain axis, 2 and 3. Comparing the first and second columns of *Table 3* indicates that the inclusion of the vibrational free energy also results in a decrease in the elastic stiffness along the axial direction and an increase in stiffness transverse to the chain. This effect is dependent on temperature as shown in *Table 2*. Comparison of the potential energy contributions reported in *Table 3* to the values reported by Karasawa and Goddard[14] using the original MSXX force field indicates that the primary effect of the modified fluorine van der Waals parameters is to reduce the anisotropy between C_{22} and C_{33} in the *ab* plane. As seen in *Table 3*, the introduction of the vibrational free energy contribution to C_{ij} serves to further attenuate this anisotropy. These results are consistent with observations made by Tashiro *et al.*[12] that, based on X-ray diffraction measurements, there is little anisotropy in the modulus of β-PVDF in the *ab* plane normal to the chain axis.

Table 2 Calculated properties of β-PVDF at several temperatures

		0 K	100 K	200 K	300 K	400 K
Polarization (Cm^{-2})	P_3	0.182	0.180	0.176	0.172	0.166
Unit cell parameters (Å)	a	8.385	8.414	8.477	8.552	8.652
	b	4.611	4.624	4.651	4.683	4.721
	c	2.552	2.551	2.550	2.549	2.547
and unit cell volume ($Å^3$)	V	98.7	99.2	100.5	102.1	104.0
Thermal expansion coefficients ($10^{-5}\,K^{-1}$)	α_1	0.00	−0.25	−0.33	−0.38	−0.47
	α_2	0.00	3.34	5.43	6.56	7.75
	α_3	0.00	2.81	4.32	5.13	5.84
Elastic stiffness constants (GPa)	C_{11}	293	290	285	276	265
	C_{22}	31.0	28.9	28.2	24.5	20.5
	C_{33}	32.9	31.5	29.1	26.1	22.1
	C_{12}	4.7	5.9	6.5	7.6	9.4
	C_{13}	8.5	8.6	8.7	9.1	10.1
	C_{23}	2.9	2.6	1.9	1.2	−2.1
Pyroelectric coefficient ($10^{-5}\,Cm^{-2}\,K^{-1}$)	p_3^σ	0.00	−1.91	−2.77	−3.26	−3.77
Direct piezoelectric stress coefficients ($C\,m^{-2}$)	g_{31}	−0.09	−0.09	−0.08	−0.08	−0.08
	g_{32}	−0.26	−0.27	−0.26	−0.26	−0.27
	g_{33}	−0.25	−0.25	−0.25	−0.24	−0.24
Direct piezoelectric strain coefficients ($pC\,N^{-1}$)	d_{31}	0.03	0.09	0.15	0.28	0.70
	d_{32}	−7.92	−8.57	−8.89	−10.25	−14.58
	d_{33}	−6.87	−7.22	−7.94	−9.06	−12.71

Table 3 Contributions to the elastic stiffness tensor of β-PVDF (GPa) at 300 K

	$\frac{1}{V}\left(\frac{\partial^2 U}{\partial\epsilon_i\,\partial\epsilon_j}\right)_{\text{MSXX}'}$	$\frac{1}{V}\left(\frac{\partial^2 A_{\text{vib}}}{\partial\epsilon_i\,\partial\epsilon_j}\right)_{\text{MSXX}'}$
C_{11}	281	−5.0
C_{22}	17.0	8.0
C_{33}	22.1	4.0
C_{12}	2.4	5.2
C_{13}	4.6	4.5
C_{23}	1.6	−0.4

Table 4 Contributions to the direct piezoelectric stress coefficient, g_{3i} ($C\,m^{-1}$), at 300 K

i	$\frac{2\mu^{\text{sc}}}{V}\left(\frac{\partial\langle\cos\varphi\rangle}{\partial\epsilon_i}\right)$	$\frac{2}{V}\left(\frac{\partial\Delta\mu}{\partial\epsilon_i}\right)$
1	0.00	0.09
2	−0.02	−0.07
3	0.00	−0.07

Piezoelectric stress coefficients, g_{3i}

Values for the direct piezoelectric stress coefficients, $g_{3i}, i = 1, 2, 3$, computed from equation (22) are reported in *Table 2*. All three of the coefficients are negative, indicating a decrease in polarization with strain. None of the coefficients are significantly affected by temperature. Like the elastic constants, there is significant anisotropy in the piezoelectric stress coefficients, with the coefficients transverse to the chain axis, g_{32} and g_{33}, approximately three times as large as g_{31}.

In equation (22) g_{3i} is shown to be directly proportional to the negative of the polarization, $-P_3$. This term arises from the partial derivative of the reciprocal volume with strain ($\partial(1/V)/\partial\epsilon_i = -1/V$). If the only mechanism responsible for the piezeoelectric stress response was a change in volume with strain, then the three principle coefficients would be identical and equal to the negative of the polarization. Anisotropy among the g_{3i} coefficients arises from changes in the repeat unit dipole with strain. At 300 K, we find a value for the total polarization, P_3 of $0.172\,C\,m^{-2}$ and a value of g_{33} of $-0.25\,C\,m^{-2}$, indicating a contribution from the volume effect of approximately 70%. Purvis and Taylor, using a point dipole model, found a value for P_3 of 0.086 and g_{33} of −0.28, indicating a contribution of the volume effect of only 30%. Using a fixed charge model, Al-Jishi and Taylor predicted a value for P_3 of 0.127 and g_{33} of −0.44, still indicating a contribution of the volume effect of 30%. These variations demonstrate that the crystal polarization as well as the piezoelectric stress coefficients are sensitive to the details of the repeat unit charge distribution.

As indicated in equation (22), changes in the repeat unit dipole with strain arise from two sources: changes in induced moment, and changes in amplitude of dipole oscillation. These contributions at 300 K are summarized in *Table 4*. The observed anisotropy arises primarily from changes in the induced moment, with much smaller effects due to dipole oscillations. The only non-zero contribution from changes in the dipole oscillations arises when strains are applied along 2. Positive strains along 2 move the chains farther apart along the a axis, allowing for a greater amplitude, φ, of dipole oscillations and a concomitant decrease in $\langle\cos\varphi\rangle$. For g_{32} and g_{33} changes in the induced moment results in a 30% increase over that associated with the equilibrium polarization; the induced dipole moment is reduced through the applications of positive strains along 2 and 3. This is in contrast to strain applied along 1 where the induced dipole *increases* with positive strain and g_{31} is reduced by 50% from its value assuming only expansion of volume with strain.

As discussed in Paper I, there are two contributions to the local electric field acting on a repeat unit dipole in the crystal. The first is the electric field arising from the other dipoles on the same chain. This field is opposite in

direction to the repeat unit dipole and therefore acts to reduce or depolarize the repeat unit dipole. The second is the electric field arising from the dipoles on the neighbouring chains. This field is parallel to the repeat unit dipole and acts to increase or polarize the repeat unit dipole. These two contributions to the local electric field are also manifested in the piezoelectric stress response. Positive strains along 2 and 3 move the chains farther apart, reducing the magnitude of the polarizing contribution to the local electric field and reducing the repeat unit dipole. Positive strains along 1 move the dipoles along the chain farther apart reducing the magnitude of the depolarizing contribution to the local electric field and increasing the repeat unit dipole.

Piezoelectric strain coefficients, d_{3i}

Values for the direct piezoelectric strain coefficients, d_{3i}, $i = 1, 2, 3$, computed using equation (17), are listed in *Table 2*. In *Figures 2–4* we give the relative contributions to d_{3i} expressed as the product of g_{3j} and S_{ij}. The results for d_{3i} are similar to those for g_{3i} in that there is significant anisotropy, with the coefficients transverse to the chain much larger in magnitude and opposite in sign relative to the axial coefficient. Unlike the values of g_{3i}, however, the values of d_{3i} are sensitive to temperature. This effect is due almost entirely to changes in the compliance with temperature. d_{31}, although significantly smaller than d_{32} and d_{33}, has the greatest sensitivity to temperature, increasing by more than a factor of two between 0 and 400 K. This change is due to the increasingly negative off diagonal terms of the compliance tensor, S_{21} and S_{31}. d_{32} and d_{33} are dominated by the products $g_{32}S_{22}$ and $g_{33}S_{33}$, respectively. The temperature dependencies of d_{32} and d_{33} likewise reflects those of S_{22} and S_{33}; each increases by more than 50% between 0 and 400 K.

The piezoelectric properties of semi-crystalline β-PVDF films have been extensively characterized. Kepler and Anderson report typical values of

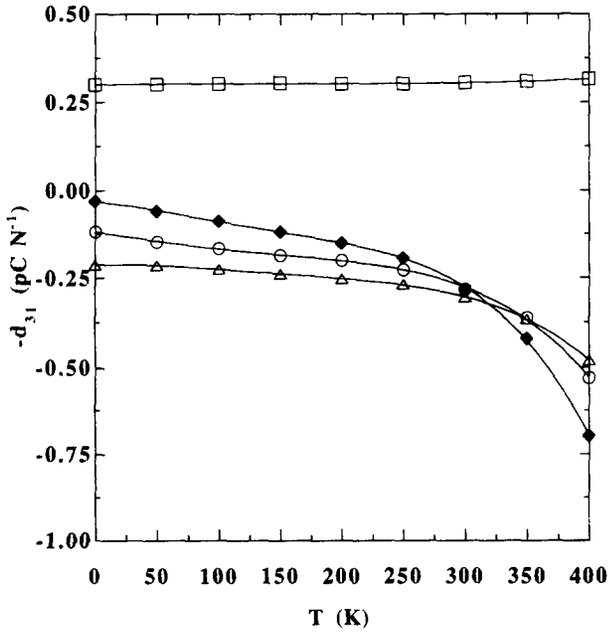

Figure 2 Direct piezoelectric strain coefficient, d_{31} (pC N^{-1}), as a function of temperature. □, $g_{31}S_{11}$; ○, $g_{32}S_{21}$; △, $g_{33}S_{31}$; ◆, total

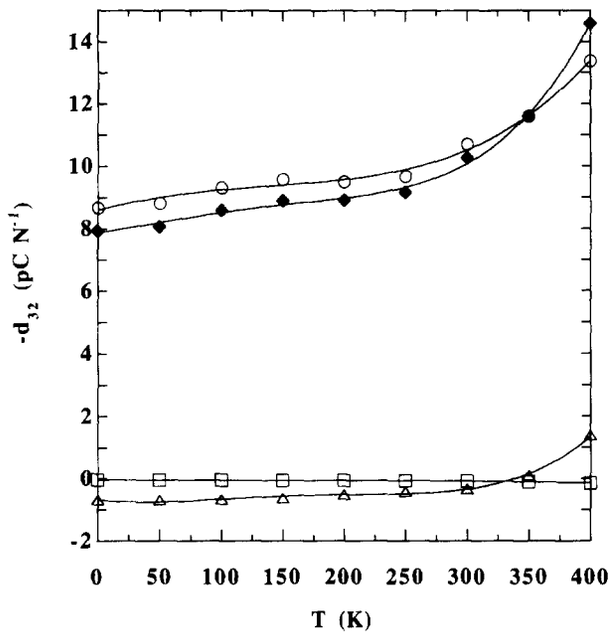

Figure 3 Direct piezoelectric strain coefficient, d_{32} (pC N^{-1}), as a function of temperature. □, $g_{31}S_{12}$; ○, $g_{32}S_{22}$; △, $g_{33}S_{32}$; ◆, total

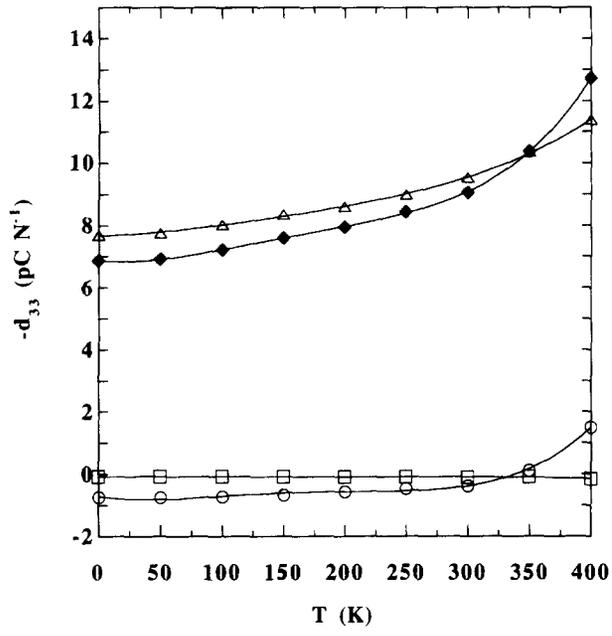

Figure 4 Direct piezoelectric strain coefficient, d_{33} (pC N^{-1}), as a function of temperature. □, $g_{31}S_{13}$; ○, $g_{32}S_{23}$; △, $g_{33}S_{33}$; ◆, total

$d_{31} = 21.4$, $d_{32} = 2.3$ and $d_{33} = -31.5\,\text{pC N}^{-1}$. A value for d_{33} of $-20 \pm 5\,\text{pC N}^{-1}$ for the crystalline phase of β-PVDF based on X-ray diffraction has been reported[12]. Our calculated value for d_{33} at 300 K is a factor of two smaller. The magnitude of this value depends directly on the transverse elastic compliance constant, S_{33}, which is in turn dependent on our choice of van der Waals parameters, as discussed previously. To further examine the effects of the van der Waals parameterization, we calculated S_{33} using both the MSXX* and the original MSXX force fields. Using the MSXX* force field and neglecting the vibrational free energy results in $S_{33}^{\text{MSXX*}} = 4.5 \times 10^{-11}\,\text{Pa}^{-1}$, giving a value of $g_{33}S_{33}^{\text{MSXX*}} = -11.4\,\text{pC N}^{-1}$. Including the vibrational free energy gives a

smaller value of $g_{33}S_{33}^{MSXX'} = -9.5\,pC\,N^{-1}$. Using the original MSXX force field and neglecting the vibrational free energy results in $S_{33}^{MSXX} = 8.3 \times 10^{-11}\,Pa^{-1}$, giving a value of $g_{33}S_{33}^{MSXX} = -21.7\,pC\,N^{-1}$ in good agreement with experiment. Although the inclusion of the vibrational free energy reduces the calculated value of d_{33} somewhat, the choice of van der Waals parameters has much more significant effect, varying d_{33} by a factor of two.

Direct vs converse piezoelectricity

In highly deformable crystals with finite polarization in the absence of applied stress, Anderson and Kepler[22] demonstrated that the correct Maxwell's relation between the direct and converse piezoelectric strain coefficients is

$$\left(\frac{\partial P_k}{\partial \sigma_i}\right)_{T,E} + \frac{P_k}{A_k}\left(\frac{\partial A_k}{\partial \sigma_i}\right)_{T,E} = \left(\frac{\partial \epsilon_i}{\partial E_k}\right)_{T,\sigma} \qquad (27)$$

where A_k is the unit cell area normal to the kth cartesian axis and P_k is the polarization at zero applied stress. For an orthorhombic crystal like β-PVDF, this relation can be written as

$$d_{ki} = d_{ik}^{c} - P_k \sum_{j=1(j\neq k)}^{3} S_{ji} \qquad (28)$$

The difference in the direct and converse coefficients is seen to arise from the product of the unit cell polarization at zero applied stress and the elastic compliance. In *Table 5* we report the direct and converse piezoelectric strain coefficients. The difference between the direct and converse coefficients is most pronounced for d_{32}. This difference is primarily a result of the term P_3S_{22}. The converse coefficients d_{32}^{c} and d_{33}^{c} also demonstrate greater anisotropy than the direct coefficients d_{32} and d_{33}. These results further demonstrate the importance of elasticity in understanding the piezoelectric response of β-PVDF.

Pyroelectricity, p_3^{σ}

The primary and secondary contributions to the pyroelectric coefficient, p_3^{σ}, as a function of temperature are given in *Table 6*. The primary and secondary pyroelectric coefficients are also plotted in *Figure 5* as a function of temperature. In contrast to the piezoelectric coefficients, the pyroelectric response goes to zero at 0 K. Above 50 K, the primary pyroelectric response is approximately constant. The negative values of the primary contribution to p_3^{σ} shown in column 1 of *Table 6* indicate an increase in the amplitude of dipole oscillation, φ, with temperature. The secondary response is sensitive to temperature. This temperature dependence reflects that of the thermal expansion coefficients. At 100 K, the primary response accounts for 17% of the total response. This contribution drops to 9% of the total response at 300 K. The experimentally determined value for p_3^{σ} for semi-crystalline uniaxially oriented films is $-2.75 \times 10^{-5}\,C\,m^{-2}\,K^{-1}$ [23]. However, one-third to one-half of this measured value is due to reversible changes in the degree of order in the semi-crystalline film[3]. Because the average degree of crystallinity is also about 50%, $-2.75 \times 10^{-5}\,C\,m^{-2}\,K^{-1}$ is probably a reasonable estimate of p_3^{σ} for the crystalline phase. This is in reasonable agreement with our calculated value of $-3.26 \times 10^{-5}\,C\,m^{-2}\,K^{-1}$. Our calculation of the contribution of primary pyroelectricity is also in agreement with the reasoning of Kepler and Anderson that primary pyroelectricity can contribute no more than 15% of the total[23].

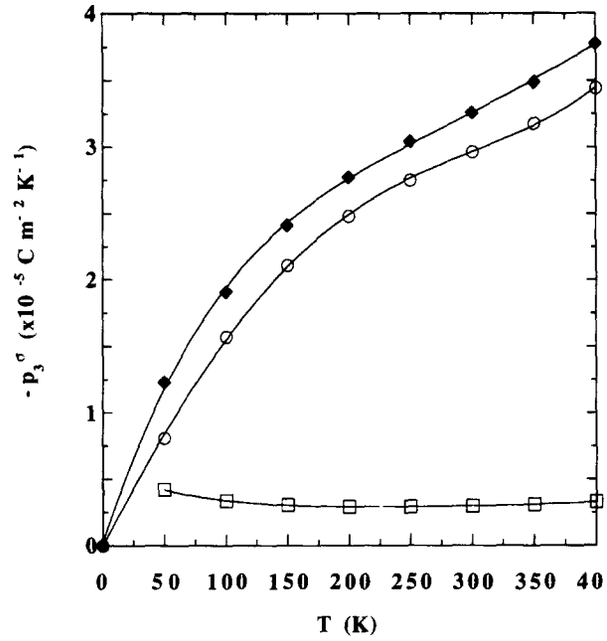

Figure 5 The constant stress pyroelectric response as a function of temperature. □, primary pyroelectricity; ○, secondary pyroelectricity; ◆, total

Table 5 Direct and converse piezoelectric strain coefficients, (pC N^{-1})

i	d_{3i}	PS_{i1}	PS_{i2}	d_{3i}^{c}
1	0.28	0.64	−0.19	0.73
2	−10.25	−0.19	6.95	−3.49
3	−9.06	−0.21	−0.24	−9.50

Table 6 Primary and secondary contributions to the pyroelectric coefficient, $p_3 \times 10^5$ (C m^2 K^{-1}), at several temperatures

T	$\frac{2\mu^{sc}}{V}\left(\frac{\partial\langle\cos\varphi\rangle}{\partial T}\right)_{\epsilon}$	$\alpha_1 g_{31}$	$\alpha_2 g_{32}$	$\alpha_3 g_{33}$	p_3
0	0.00	0.00	0.00	0.00	0.00
100	−0.34	0.02	−0.89	−0.70	−1.91
200	−0.29	0.03	−1.44	−1.07	−2.77
300	−0.30	0.03	−1.73	−1.26	−3.26
400	−0.33	0.04	−2.06	−1.42	−3.77

CONCLUSIONS

The results of our calculations on β-PVDF demonstrate that the piezoelectric stress tensor is highly anisotropic with g_{31} a factor of three less than g_{32} and g_{33}. Dipole oscillations contribute little to the piezoelectric stress coefficients and the observed anisotropy is, therefore, due to changes in the induced moment with strain. Changes in induced moment with strain are, in turn, due to changes in the local electric field.

The piezoelectric stress coefficients show little

variation with temperature. The direct piezoelectric strain tensor also shows anisotropy, with d_{31} smaller by an order of magnitude and opposite in sign to d_{32} and d_{33}. The temperature dependencies of d_{3i} are significant and are determined by the temperature dependence of the elastic compliance constants. The predicted values also reflect the sensitivity of the elastic compliance constants to small differences in the van der Waals parameterization. The Maxwell relation between the direct and converse piezoelectric strain coefficients given by Kepler and Anderson is confirmed with differences of as much as a factor of three found. Finally, the calculated pyroelectric response, p_3, of the crystal is comparable to that reported for semi-crystalline films. Primary pyroelectricity accounts for about 9% of the total response of the crystal at 300 K. The temperature dependence of secondary pyroelectricity is significant and determined by that of the thermal expansion coefficients.

ACKNOWLEDGEMENTS

The authors would like to acknowledge D. J. Lacks for his helpful comments and are grateful to the AT&T Foundation and to the National Science Foundation (CTS 9457111) for financial support of this work.

REFERENCES

1 Lovinger, A. 'Developments in Crystalline Polymers', Vol. 1, Applied Sciences, London, 1981
2 Wang, T., Herbert, J. and Glass, A. 'The Applications of Ferroelectric Polymers', Blackie, Glasgow, 1988
3 Kepler, R. and Anderson, R. *Adv. Phys.* 1992, **41**, 1
4 Capron, B. and Hess, D. *IEEE Trans.* 1986, **UFFC-33**, 33
5 Nye, J. 'Physical Properties of Crystals', Oxford Press, Oxford, 1985
6 Broadhurst, M., Davis, J., McKinney, G. T. and Collins, R. *J. Appl. Phys.* 1978, **49**, 4992
7 Purvis, C. and Taylor, P. *Phys. Rev. B* 1982, **26**, 4547
8 Purvis, C. and Taylor, P. *Phys. Rev. B* 1982, **26**, 4564
9 Purvis, C. and Taylor, P. *J. Appl. Phys.* 1983, **54**, 1021
10 Al-Jishi, R. and Taylor, P. *J. Appl. Phys.* 1985, **57**, 897
11 Al-Jishi, R. and Taylor, P. *J. Appl. Phys.* 1985, **57**, 902
12 Tashiro, K., Kobayashi, M., Tadokoro, H. and Fukada, E. *Macromolecules* 1980, **13**, 691
13 Tashiro, K., Tadokoro, H. and Kobayashi, M. *Ferroelectrics* 1981, **32**, 167
14 Karasawa, N. and Goddard, W. *Macromolecules* 1992, **25**, 7268
15 Carbeck, J., Lacks, D. and Rutledge, G. *J. Chem. Phys.*, 1995, **103**(23), 10347
16 Born, M. and Huang, K. 'Dynamical Theory of Crystal Lattices', Oxford Press, Oxford, 1954
17 Venkataraman, G., Feldkamp, L. and Sahni, V. 'Dynamics of Perfect Crystals', MIT Press, Cambridge, 1975
18 Lacks, D. and Rutledge, G. *J. Phys. Chem.* 1994, **98**, 1222
19 Murthy, C., Singer, K. and McDonald, I. in 'Advances in Chemistry Series', Vol. 204, American Chemical Society, Washington DC., 1983, Chap. 9
20 Karasawa, N. and Goddard, W. *J. Phys. Chem.* 1989, **93**, 7320
21 Kepler, R. and Anderson, R. *J. Appl. Phys.* 1978, **49**, 4490
22 Andersen, R. and Kepler, R. *Ferroelectrics* 1981, **32**, 13
23 Kepler, R. and Anderson, R. *Mol. Cryst. Liq. Cryst.* 1984, **106**, 345

APPENDIX: CALCULATION OF THE TEMPERATURE AND STRAIN DERIVATIVES OF $\langle\cos\varphi\rangle$

In a previous publication[15] we compared our CLD calculations to molecular dynamics simulations and demonstrated that the root-mean-squared amplitude of oscillation, φ_{RMS}, of the repeat unit dipole could be estimated accurately up to 300 K by assuming harmonic oscillation

$$\varphi_{RMS} = 1/\omega_{B_2}\sqrt{E_{vib}^{B_2}/I} \tag{A1}$$

where ω_{B_2} is the frequency of the rotational lattice mode with B_2 symmetry. $I = 1.31 \times 10^{-45}\,kg\,m^{-2}$ is the moment of inertia of a repeat unit of β-PVDF rotating about an axis parallel to the c axis and passing through the chain centre of mass.

For temperatures less than the vibrational temperature, defined as $\hbar\omega_{B_2}/k_B$, quantum mechanical effects become significant. For ω_{B_2} the vibrational temperature is approximately 130 K. Because we are interested in the crystal properties from 0 K, we use the quantum mechanical expression for the thermodynamic energy of a harmonic oscillator

$$E_{vib}^{B_2} = \frac{\hbar\omega_{B_2}}{2} + \hbar\omega_{B_2}\left[\exp\left(\frac{\hbar\omega_{B_2}}{k_b T}\right) - 1\right]^{-1} \tag{A2}$$

For values of $\varphi_{RMS} < 20°$, observed here, $\langle\cos\varphi\rangle \approx \cos\varphi_{RMS}$.

In the quasi-harmonic approximation, changes in the normal-mode frequencies arise solely from changes in the lattice constants. In the primary pyroelectric

Table A1 Contributions to the derivative of $\langle\cos\varphi\rangle$

	0 K	100 K	200 K	300 K	400 K
ω_{B_2} cm^{-1}	97.28	94.86	89.75	83.91	76.82
$E_{vib}^{B_2}/kT$	—	1.83	1.36	1.21	1.14
φ_{RMS}	2.69	4.46	5.73	7.10	8.70
$\langle\cos\varphi\rangle$	0.999	0.997	0.995	0.992	0.988
$\frac{\partial\omega_{B_2}}{\partial\epsilon_1}$ cm^{-1}	−331	−322	−304	−282	−255
$\frac{\partial\omega_{B_2}}{\partial\epsilon_2}$ cm^{-1}	−1162	−1146	−1111	−1068	−1013
$\frac{\partial\omega_{B_2}}{\partial\epsilon_3}$ cm^{-1}	−345	−336	−317	−297	−272

response, the lattice constants and, therefore ω_{B_2}, are fixed. The partial derivative of $\langle\cos\varphi\rangle$ with T at constant strain is thus

$$\left(\frac{\partial\langle\cos\varphi\rangle}{\partial T}\right)_{\epsilon} = -\sin\varphi_{\mathrm{RMS}}\left[\frac{1}{\omega_{B_2}}\left(\frac{\partial\sqrt{E_{\mathrm{vib}}^{B_2}/I}}{\partial T}\right)_{\epsilon}\right] \quad \text{(A3)}$$

The partial derivative of $\langle\cos\varphi\rangle$ with ϵ at constant T is

$$\left(\frac{\partial\langle\cos\varphi\rangle}{\partial\epsilon_i}\right) = -\sin\varphi_{\mathrm{RMS}}\left[-\frac{1}{\omega_{B_2}^2}\sqrt{\frac{E_{\mathrm{vib}}^{B_2}}{I}}\left(\frac{\partial\omega_{B_2}}{\partial\omega_i}\right)\right.$$

$$\left.+\frac{1}{\omega_{B_2}}\left(\frac{\partial\sqrt{E_{\mathrm{vib}}^{B_2}/I}}{\partial\omega_{B_2}}\right)\left(\frac{\partial\omega_{B_2}}{\partial\epsilon_i}\right)\right] \quad \text{(A4)}$$

From CLD we obtain ω_{B_2} and its derivative with strain. $E_{\mathrm{vib}}^{B_2}$ and the derivative of $\sqrt{E_{\mathrm{vib}}^{B_2}/I}$ with T at constant strain are obtained directly from equation (A2). The derivative of $\sqrt{E_{\mathrm{vib}}^{B_2}/I}$ with ϵ is evaluated numerically and φ_{RMS} is calculated from equation (A1). Values for ω_{B_2}, $E_{\mathrm{vib}}^{B_2}$, φ_{RMS}, $\langle\cos\varphi\rangle$ and $\partial\omega_{B_2}/\partial\epsilon_i$ are given in *Table A1*.